PHASE RELATIONSHIPS IN THE Mo-(Fe, Co, Ni)-Si TERNARY SYSTEMS NEAR THE TRANSITION METAL BINARIES

BY
JOGENDER SINGH

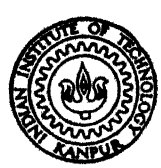

DEPARTMENT OF METALLURGICAL ENGINEERING
INDIAN INSTITUTE OF TECHNOLOGY KANPUR
JULY, 1976

PHASE RELATIONSHIPS IN THE Mo-(Fe, Co, Ni)-Si TERNARY SYSTEMS NEAR THE TRANSITION METAL BINARIES

A Thesis Submitted
in Partial Fulfilment of the Requirements
for the Degree of
MASTER OF TECHNOLOGY

BY
JOGENDER SINGH

to the

DEPARTMENT OF METALLURGICAL ENGINEERING
INDIAN INSTITUTE OF TECHNOLOGY KANPUR
JULY, 1976

C E R T I F I C A T E

This is to certify that this work on "Phase Relationships in the Mo-(Fe,Co,Ni)-Si Ternary systems Near the Transition Metal Binaries'' has been carried out under my supervision and it has not been submitted elsewhere for a degree.

(Dr. K.P. Gupta)
Professor
Department of Metallurgical Engineering
Indian Institute of Technology
KANPUR.

ME-1976-M-SIN-PHA

CONTENTS

CHAPTER I

INTRODUCTION

Modern advances in deep sea and deep space exploration and in aviation fields have given birth to a number of super-alloys which contains among other elements refractory transition elements such as Nb, Ta, Mo, W or Ti. For successful development of these alloys (which are usually multi component) a thorough knowledge of the phase relationships in the various alloy systems is required, especially because many of the transition metal alloy systems produce extremely brittle phases. The presence of these brittle phases are detrimental to the mechanical properties of alloys.

Electronic structure of the transition elements and their alloy chemistry are complex. Proper understanding of alloying behaviour of transition elements is possible to obtain through the study of phase relationships in the alloy systems of these elements. There are several phases with complex crystal structures that occur in the transition metal alloy systems. Some of these are the σ , μ , , R, P, Cr_3O type , Ti_2Ni type, Laves phases

etc. The structural and other characteristics of some of these phases are shown in Table I. Most of these phases appear in binary and ternary systems and some appear only in the ternary systems. Among the phases which appear in the binary systems, the σ, μ, and phases are of variable stoichiometry where as the Cr_3O type, Ti_2Ni type, and Laves phases are of fixed stoichiometry[1]. R and P phases usually occur in the ternary systems. (R phase has been recently observed in Mn-Ti[2] and Mn-S_i[3] systems). The study of the alloying behaviour of transition elements seems to indicate that in the binary and ternary systems two important factors govern the occurence of intermediate phases, namely, the valence electron concentration and the atomic size[4]. The electronic factor seems to be responsible for introducing a selectivity in the choice of A and B components and a systematic shift of the mean composition of the phase region, as is observed for the σ phases[5]. Usually, the line dividing the A and B elements appear near the Mn group elements in the periodic table. The elements to the left of the Mn group behave as the A component and those to the right of the Mn group elements (including the Mn group elements) behave as the B component. On the other hand, the atomic size factor appears to follow an efficient space filling condition[6,7] and the stability

of phases of fixed stoichiometry have been attributed variously to atomic size factor. It has been, however, realised that none of these factors work alone in the formation or stabilization of a phase. From the Table I, it is clear that as far as the transition element compounds are concerned, the R_A/R_B and e/a ranges overlap for most of the phases. The σ, μ, R, P etc. appear to be stable over a narrow overlapping range of electron: atom ratio (e/a) of 5.6 to 8.0[5] and R_A/R_B is very close to 1.0. Information on the relative stability of these phases can be obtained from a limited number of ternary systems studied. Some of these clearly show that while the extension of a phase region in a certain direction occur due to favourable e/a size factor limits its extension in other directions. A typical example is the large extension of the α-Mn phase as a narrow phase field along a constant Ti line in the Ti-Mn-Fe system (favourable e/a) whereas no extension of the same phase is found in the direction of increasing Ti[8] (size effect).

One of the structural characteristics of the transition metal electron compounds is that all of them posses more than one type of sites of high coordiation number (CN)[1,7], namely CN16, CN15, CN14 (or CN13) and CN12. The volume associated with these high coordination sites

increases with increasing CN and all these phases show site preference ordering of large and small size atom in the large and small volume sites, respectively[7].

While, inspite of favourable size and electronic factors, the transition element binaries do not always contain the σ[9], or R[9,10] intermediate phases, the ternary systems involving the same transition elements many a times show the presence of the σ[8], R[8,9] phases. This is referred to in the literature as the stabilization of the intermediate phases. Stabilization phenomena is not restricted only to the systems involving only transition elements but is found to occur for various ternary systems of transition elements with non-transition elements. Typical example of this is the stabilization of the σ[11,12], R[13] and Laves phases[14] by Si.

The effect of stabilization of complex phases by Si has been observed in various ternary systems involving transition elements of the first long period. For the refractory transition metals, however, very little systematic phase equilibria work exists to date. As a part of a detailed investigation in the RT-(Fe, Co, Ni)-Si ternary systems, where RT stands for refractory transition elements Nb, Ta, Mo and W, in the present investigation Mo has been choosen as the refractory transition metal.

Among the three transition metal binary systems Mo-Fe, Mo-Co, and Mo-Ni, the first two appear to be quite similar. In both the Mo-Co and Mo-Fe systems, Fig. 1 and 2, the μ phase exists from room temperature to high temperature as a narrow phase field. In the Mo-Fe system the μ phase extends from 36 to 40 at pct Mo and is stable upto 1480°C. In the Mo-Co system the μ phase extends from 45 to 50 at pct Mo and is stable upto 1510°C. At a slightly higher Mo concentration the σ phase appears as a high temperature phase in both the binary diagrams. In the Mo-Fe system the σ phase is stable between 1180° to 1540°C with a triangle shaped composition range which extends from 42 to 50 at pct Mo whereas in the Mo-Co system the triangle shaped σ phase region is stable between 1250° to 1620°C in the composition range of 60 to 68 at pct Mo. A third phase $MoCo_3$ exists in the Mo-Co system and it is stable below 1000°C. On the other hand the Mo-Ni system, Fig. 3, neither shows the μ phase nor shows the σ phase. A new phase, the δ phase, appears in the composition range of 46 to 49 at pct Mo and is stable upto 1362°C. Besides the δ phase, there are two more phases, $MoNi_3$ and $MoNi_4$, which appears at the higher Ni side and are stable below 1000°C.

In the transition metal - Si systems involving Mo, Fe, Co and Ni large number of silicides occur. In

the Mo-Si system, three silicides Mo_3Si, Mo_3Si_2 and $MoSi_2$, all high melting point (2000°C) phases exist. In the (Fe,Co,Ni)-Si systems, addition of Si lowers the melting point of the alloys and eutectics occur in the three binaries at 1200°C (34 at pct Si in Fe), 1195°C (23 at pct Si in Co) and 1152°C (21.4 at pct Ni). While there are several silicides of melting points lower than 1250°C in all the three systems, the only silicides which exists above 1250°C are FeSi (M.P. = 1410°C), Co_2Si (M.P. = 1332°C) and Ni_5Si_2 (M.P. = 1282°C) and Ni_2Si (M.P. = 1318°C).

Mo-(Fe, Co, Ni)-Si systems have been studied in the past in a cursory manner. Kuzma et al[15] studied the Mo-(Fe, Co, Ni)-Si systems at 800°C and 1000°C. In all the three systems these workers found the presence of $MgZn_2$ type Laves phase near equiatomic composition (ABC). However, the phase regions were not determined. Bardos et al[14] also found that the $MgZn_2$ type Laves phases exist at the $A_2(B_3C)$ composition in the Mo-(Co,Ni)-Si systems even though no binary Laves phase exists in either of the two transition metal binary systems. Recently the Mo-Ni-Si system has been studied by Raman et al[16] at 900°C. In their limited Si content phase equilibria study, they have discovered ternary R and μ phases in the Mo-Ni-Si system. The R phase occurs as a narrow region between 2 to 17

at % Si and 51 to 58 at pct Mo. The μ phase appears as a 'V' shaped region with approximately 48 at pct Mo and 8 at pct Si. No detailed study, however, is available for the Mo-(Fe,Co)-Si systems.

In the present investigation the Mo-(Fe,Co,Ni)-Si ternary systems have been studied at a relatively high temperature and relatively low Si contents. Since the σ phase exists above 1250° and 1180°C in the Mo-Co and Mo-Fe systems, respectively, to study the relative stability of the σ and μ phases, isothermal annealing temperature of 1280°C was chosen for the Mo-(Fe,Co)-Si systems. For convenience of using only one annealing furnace the Mo-Ni-Si system also has been studied at the same temperature. The 1280°C isothermal section of the Mo-(Fe,Co,Ni)-Si systems were investigated upto 34 at pct Si.

CHAPTER II

EXPERIMENTAL PROCEDURE

The experimental work for the investigation of the ternary systems Mo-(Fe,Co,Ni)-Si involves the following steps:

(A) Melting

(B) Annealing

(C) Metallographic analysis and

(D) X-ray diffraction analysis.

The material used in the present work are 99.9% pure Mo powder, electrolytic Fe, Co, Si of 99.9% purity supplied by Semi Elements Inc. New York and 99.9% pure Ni supplied by Gallard Schelsinger Mfg. Co., New York. Mo was available in the powder form and was not suitable for use in an arc melting furnace. 0.94 cm dia x 0.2 cm to 0.7 cm Mo pallets were made by pressing Mo powder in a die using a small hydraulic press. The pressure used was between 1500 to 1700 psi. Co was in bar or rod form and it was cut to a suitable size. Fe and Ni were in the chip form. A 10 gm charge of each alloy was prepared. Very small particles were avoided because they tended to scatter around and were lost when arc struck the charge.

(A) Melting:

Melting of the alloys was done in a non-consumable Tungeston electrode water cooled copper hearth D.C. electric arc furnace under argon atmosphere. A great care was exercised during melting for obtaining high purity alloys. A definite charging sequence was followed to bring the melting loss of the alloys to a minimum. The copper crucible was cleaned up using emery paper and with acetone before putting the component elements. Fe, Co or Ni was placed as the first layer on the copper crucible, and Si was charged on the top of this layer. Mo pellet was placed on top so as to produce a smooth top surface and to strike the arc on the high melting point component. Care was taken that Mo pellet was in contact with the bottom layer of Fe, Co, or Ni and the contacts were not broken by Si layer. This heap of charge ensured the arc to strike at the centre of the charge. Mo melted and in turn dissolved the low melting point components Fe, Co, Ni and Si, thereby minimizing losses. The maximum loss in melting was less than 2%. The time for melting was set for 15 seconds. After each melting the alloy was broken into pieces and the furnace was recharged with the pieces keeping them up side down and with the peripheral parts towards the centre of the crucible. Each alloy was melted in this

manner three to four times to ensure homogeneous alloy. Since the loss was consistent and small no alloys were chemically analysed.

(B) Annealing:

For annealing the cast alloys were broken into pieces of suitable sizes. The surface of the piece to be annealed was ground to remove any oxide that might have formed, sealed in an evacuated fused silica tube and annealed in a vertical tube Globar furnace at 1280°C. The furnace temperature was controlled within ± 2°C. Each alloy was annealed for 96 hours and subsequently quenched in tap water. In case of any power failure during annealing, the specimens were removed from the furnace without quenching, the furnace temperature was reset and specimens were reannealed. Since in a batch, five to six samples were annealed, care was taken to properly identify the specimens. The shape of each specimen was noted and each capsule was identified by putting a number of Kanthal wire identification rings on the capsule.

(C) Metallographic Analysis

The surface of each annealed specimens were ground off and each piece was broken into two parts, one was used for metallographic examination and the other

for X-ray diffraction work. For metallographic examination a piece of each alloy was mounted in lucite and polished on emery papers, 1/0 through 4/0, followed by polishing on Microcloth covered wheel. 0.5 micron Al_2O_3 powder suspened in water was used as the polishing abresive. After polishing, the specimens were thoroughly washed with water and dried by a high speed air blower. The specimens were checked under a microscope in the as polished condition to detect the presence of inhomogeneity and oxides. The polished specimens were then etched to reveal the microstructure. The etching reagents used consisted of HF acid, HNO_3 and H_2O in the ratio of 4 c.c. : 1 c.c. : 1 c.c. for the Mo-(Fe,Ni)-Si alloys and in the ratio of 4 c.c. : 1 c.c. : 2 c.c. for the Mo-Co-Si alloys.

(D) X-ray Diffraction Analysis:

After removing the surface layer by grinding a piece of each annealed alloy was used for preparing powder for X-ray diffraction work. The alloys were brittle and so it was easy to prepare - -300 mesh powder using steel and agate mortars and pastles. For phase identification purposes the brittle nature of the specimen did not necessitate annealing of the powders for removal of stresses. Because of its higher resolving power and lower exposure

time compared to a Debye Scherrer camera, a 20 cm dia asymmetrical focusing camera was used for phase identification work. Typical exposure time for the asymmetrical focusing camera was just 4 hours. The specimen for the asymmetrical focusing camera was prepared by spreading a uniformly thin layer of powder on a small piece of computer data card coated with Krylon clear plastic spray and then recoating it with the same plastic spray. The first layer of plastic spray held the powder on the card and both the layers of the sprayed material saved the powder from atmospheric oxidation. The specimen thus prepared could be kept for a long period of time without oxidation of the powder specimen.

For indexing the single phase alloy powder patterns, a 114.6 mm. dia Debye-Scherrer camera was used. Before preparing the specimens for the Debye-Scherrer camera the alloy powders were annealed at 1280°C for 20 minutes to remove the residual stresses. Evacuated and scaled quartz capsules were used for powder annealing. The specimens were made by sealing the annealed powder in thin plastic tubes. For all X-ray diffraction work unfiltered Cr radiation at 30 kv and 15 mA was used. The typical exposure time for the 114.6 mm dia Debye-Scherrer camera was 12 hours.

CHAPTER III

RESULTS AND DISCUSSION

The isothermal section of the ternary systems Mo-(Fe,Co,Ni)-Si were studied at 1280°C. The phase analysis of the alloys was done through metallographic and X-ray diffraction techniques and are shown in Table II to IV. The phase relationships at 1280°C for the three systems, based on the data of Table II to IV, are shown in Figs 4 to 6.

As mentioned earlier the Mo-Fe and Mo-Co systems have μ-phase and σ phase at 1280°C whereas only the δ phase is present in the Mo-Ni system. Addition of Si appears to extend the binary μ phase regions in the ternaries but the σ phase and the δ phase regions appear to be very restricted. The phase boundries of the σ and δ phases were not determined well and hence in Figs.4, 5 and 6 the possible small extensions of these phases are indicated with dashed line. In the Mo-Co-Si system the μ phase region extends as a narrow phase region along almost a contant Mo line. In the Mo-Fe-Si system, the μ phase appears to have two directions of extension, one of which is along a constant Mo line (39 at pct Mo, the mean Mo composition of the binary phase) and in the direction of increasing

Mo content. Compared to the Mo-Co-Si system the μ phase region in the Mo-Fe-Si system is reasonably wide but with smaller maximum solubility of Si. The Mo-Ni system does not have any μ phase but ternary μ phase region has been found at the 50 to 51 at pct Mo, 40 to 41 at pct Ni and 9 to 10 at pct Si composition. The Mo-Ni-Si system was investigated earlier by Raman[16] at lower temperature (900°C) and a 'V' shaped phase region with its axis almost parallel to 8 at pct Si line was observed. The composition region of the μ phase in the present investigation corresponds to the earlier investigation, indicating that the present phase region is an extension of the μ phase region found by Raman. However the μ phase at 1280°C appears to be very restricted and it may mean that the μ phase forms either through a peritectic reaction or directly from the melt.

The extension of the μ phase in the Mo-Co-Si system appears to be similar in nature to that observed in the Nb-Fe-Si and Nb-Co-Si systems. The stabilization of the μ phase in ternaries has been considered to depend on the e/a; maintainance of a constant e/a is usually considered to be the guiding factor[5]. Extension and stabilization of the μ phase on addition of Si is possibly due to the same effect maintainance of e/a and possible lowering of e/a (in the case of Mo-Ni system) to the

desired value (usual e/a range of stability of μ phase is 7.08 to 7.62 and for the Mo-Ni system it is 8) by Si. On this basis, however, it is not clear why in the Nb-Fe-Si, Nb-Co-Si and Mo-Co-Si systems the μ phase region be narrow and extend along almost constant Nb or Mo lines. The crystal structure data (Table I) of the μ phase shows that it has CN12, CN14, CN15 and CN16 sites[7]. Site preference ordering studies in the μ phases of Mo and W[7] indicate (Table V) that CN15 and CN16 sites are exclusively occupied by Mo and W, CN14 sites are preferentially occupied by Mo and W and small size atoms occupy the smaller volume CN12 sites. The number of CN14, 15, 16 sites are 6 out of total 13 atomic sites for the rhombohedrel cell. The ratio of the large size to the small size atoms is the 6:7, as is observed in the W_6Fe_7 μ phase. In the Mo-Co system the mean composition of the μ phase region is almost about Mo_6Co_7. The position of the Si atoms in the μ phase structure has not been determined any time but the μ phase may behave like the σ phase in which Si prefers the CN12 sites[12]. Thus, even if the e/a ratio remains favourable, on addition of Si in the Mo-Co μ phase, it can extend only along a constant Mo line because there is no large volume site available to accomodate Mo.

In the Mo-Fe-Si system, however, the μ phase region appears to extend in two directions, the broader

part of the phase region extending along a constant Mo line of 39 at pct Mo and the other in a direction of increasing Mo while the extension of the μ phase along the constant Mo line may be considered to be due to having favourable e/a continuing on addition of Si, whether the same effect can extend the μ phase in the direction of increasing Mo, is not known. It is to be noted, however, that the Mo-Fe μ phase appears at considerably higher Fe (B element) content. For the μ phase a large part of CN14 sites will be expected to be partially occupied by Fe. Since Mo can go into the CN14 sites easily, the structure may tolerate a change in Mo content. If this is true, then again the phase region should not extend beyond 47 at pct Mo at which all the CN14 sites will be filled by Mo. This is exactly what is observed in the Mo-Co-Si system; the μ phase region extends only upto 49 at pct Mo. It is also to be noted that the lower e/a limit of stability of the μ phase is 7.08, which occurs for the Mo-Fe system. If the general effect of Si is to lower the e/a ratio of the μ phase (as has been stated to be the cause of stabilization of the μ phase in the Mo-Ni-Si system) then addition of Si to Mo-Fe μ phase will lower the e/a below 7.08. If the lowest e/a limit of stability for the μ phase is slightly below 7.08 then one would expect that on addition of Si

the Mo-Fe μ phase may have an easy destabilization than in the Mo-Co-Si system. This is possibly the reason why the μ phase extends farther in the Mo-Co-Si system and less in Mo-Fe-Si system. The limiting e/a for the μ phase, however, can not be estimated from the present data because the exact nature of interaction of Si atom with the transition metal atoms is not known.

In some transition metal ternaries, e.g. Mo-Cr-Co, Mo-Fe-Mn, Mo-Co-Mn, the R-phase was found to occur along the same line of extension of the phase and in one case between the σ and the μ phase. Since the σ and μ phase are considered to be electron compounds, the occurence of R phase along the same line of extension of the μ phase and σ phase has been used to indicate that the R phase is also an electron compound. The R phase e/a in the above systems was found to be very similar to the μ phase, but possibly on the lower side. On the basis of our assumption that Si in general lowers the e/a of the complex phases, it is expected that an R phase may be expected after the μ phase extension stops in the Mo-(Fe,Co,Ni)-Si systems. While the Mo-Co-Si system shows the R phase (Table XII)at higher Si content than the μ phase no such R phase region could be detected in the Mo-Fe-Si system. It is possible, however, that the R

phase is not stable at the temperature of present investigation but may be found at still higher or lower temperatures. The δ phase in the Mo-Ni system is the only known structure of its kind. The study of Mo-Ni-Fe[19] and Mo-Ni-Co[19] systems again indicate that the μ phase and δ phase more or less extend along the same direction from the respective binaries and in one case (Mo-Ni-Fe) the P phase, an electron compound, is stabilised between the μ and the δ phase. If the δ phase is also an electron compound, the e/a value (e/a = 8) is greater than the μ phase. Thus an addition of Si may lower the e/a to stabilize the μ as well as the R phase. In the Mo-Ni-Si ternary the μ and R phases have been found very close to each other.

The R phase has 53 atoms per cell with 27 atoms in the CN12 sites, 12 atoms in the CN14 sites, 6 atoms in the CN15 sites and 8 atoms in the CN16 sites[20]. The site preference ordering studies by X-ray and Neutron diffraction[20] indicate that the CN16 sites are exclusively occupies by large A atoms, CN15 and CN14 sites are preferentially occupies by large A atoms along with some amount of B atoms, and CN12 sites are extensively occupied by small B atoms. The total of CN16, 15, 14 sites in the R phase structure amounts to about 49%. In the present case, the Mo-Ni-Si and Mo-Co-Si systems, R phase appear

at around 50 at pct Mo which again may mean that Mo exclusively fills the higher coordination sites.

As mentioned earlier, none of the Mo-Fe, Mo-Co and Mo-Ni binary systems show the presence of Laves phases. But on addition of Si up to 34 at pct several phases resembling the $MgZn_2$ type Laves phase appear in the three ternary systems investigated. While the main diffraction lines of the $MgZn_2$ type Laves phase appear in the diffraction patterns of all the new phases discovered, many weak to medium strong extra diffraction lines were observed in each diffraction pattern indicating that the new phases are some-what different from the $MgZn_2$ type phases. In all six Laves type phases (designated as ε_n) were found extending along the 33.3 at pct Mo lines, three in the Fe system, two each in the Co and Ni systems. The lowest Si content Laves type phase (phase ε_1) in the Fe and Co systems were found to be the same. The X-ray diffraction patterns of all the Laves type phases are shown in Table VI to XI.

In all the ternaries, the ε_n phase regions are very narrow and extend along the 33.3 at pct Mo line. In the Laves phases it has been observed that there are two types of sites available, sites with CN 16 and sites with CN12. Site preference ordering studies in Laves phases[1] indicate that the large size atoms exclusively occupy

the CN16 sites. Since there are the ratio of the CN16 : CN12 sites at the AB_2 composition is 1:2. Thus all the CN16 sites are occupied by the large A atoms. Since the atomic size of Mo is larger than the Fe,Co,Ni and Si (effective radius of Si in transition metals is known to be much smaller than the atomic radius estimated from the diamond structure of Si[21]), it is expected to go into and completely fill the CN16 sites. It has been observed that Laves phases usually do not tolerate large or small size atoms in the two types of lattice sites[22]. Hence the Laves phases are usually very narrow. The same may be true for the new types of Laves phases (ε_n) found in this investigation. In the previous investigation by Kuzma et al[15] and Bardos et al[14], the presence of $MgZr_2$ type Laves phases were reported. All these investigations were carried out at or below 1000°C. Since the Laves phase are known to show allotropy with change in temperature[1], it is possible that the present variation in Laves phase structure is due to a higher annealing temperature employed in this investigation.

The Laves phases are stoichiometric compound of formula AB_2 in which the A atoms are always larger atoms of the two. The A elements can be from anywhere in the periodic table (not considering the elements to the right of Group II B except Al). It is also found that an

element may behave as an A element with some elements, but may behave as a B element with same other elements. An important feature of the Laves phases is that for the radius ratio of $R_A/R_B = 1.225$ the A atoms are in contact with A atoms only, the B atoms are in contact with the B atoms only and no A-B contacts occur . It has been suggested[23] that the Laves phases get stabilized by adjusting the effective radius of the atoms to conform to the requirement of ideal radius ratio. On this basis the Laves phases are considered to be size compounds. If the radius ratio of two elements is close to 1.225 it is expected to form Laves phases and several Laves phases could be discovered on this basis. However, there are a large number of cases in which no Laves phase is found inspite of favourable radius ratio. Typical examples of these cases are the systems (Sc, Y, Ti, Zr, Mo, W) - (Fe, Co, Ni). Stabilization of Laves phases has been observed the some of these alloy systems when Si was added as a third element, e.g. (W, Mo) - (Fe,Co,Ni)-Si[15]. Bardos et al[14] suggested that the stabilization of Laves phases with Si is due to electronic effect. Considering the number of electrons out side the Argon core they showed that Si reduces the effective e/a to below 8, a criteria considered necessary to be fulfilled for the stabilization of the Laves phases. The stabilization of the Laves type phases found in the

present investigation can be understood on the basis of the above criteria.

Usually three types of Laves phases are observed - $MgZn_2$ (Hexegonal), $MgCu_2$ (cubic) and $MgNi_2$ (Hexagonal). It was known for a long time that the variation in the structure of Laves phases can be rationalized on the basis of variation in layer sequence. Recently Komura[24] has made a systematic study of possible variations in the layer sequences in Laves phases.

Komura[24] has broken up the Laves phase structure into small structural units, each consisting of four planes of atoms. Starting with one structural unit (layer) called A, the six possible variation of layers have been worked out, as is shown in Fig. 7. Any Laves phase structure may be constructed using several of these layers in proper sequence. The possible stacking sequence of these layers follow the scheme shown in Fig. 8. On this basis the $MgZn_2$ type phase is a two layer sequence structure with structural units arranged as AB'. Similarly, the $MgCu_2$ structure is with ABC stacking and the $MgNi_2$ structure is with AB' A'C stacking. While these three structures are predominent Komura has shown that in ternary system, involving $MgCu_2$ and $MgZn_2$ structures in two binaries, multi-layered Laves phases occur as ternary compounds. As for example, in the Mg-Cu Al system a 9

layer structure with stacking sequence ABC' BC A'C'BC'B' and a 5 layer structure with sequence ABC AB' occurs[24]. Similarly 8, 9 and 10 layer structures have been observed in the Mg-Zn-Cu and Mg-Zn-Ag systems[25].

In the present case, since the ε_1 to ε_6 phases very closely resemble the $MgZn_2$ type Laves phase but have more diffraction lines, it appears that the new Laves type phases are multilayered Laves phases. For a few of the newly discovered phases an attempt was made to determine the number of layers present in them. To determine the number of layers and hence the lattice parameters, the diffraction patterns of ε_1 and ε_3 phases were compared with an already indexed $MgZn_2$ pattern to identify some of the reflections. Using these reflections and the (hkl) indices corresponding to the $MgZn_2$ structure, lattice parameters were determined. Since the $MgZn_2$ structures is a two layer structure the height of each layer will be $c/2$. From the calculated lattice parameters (on the basis of $MgZn_2$ indexing) the layer height was determined. This gave the possible values of **c** for the multilayered Laves phases; the **c** values were calculated upto 10 layers. With these new **c** values and the already known a values, the c/a values were calculated. Indexing of the ε_1 and ε_3 patterns were tried using a Burn Chart at the different possible c/a values. The best match was noted and the d spacings were

calculated on the basis of the new indexing. The results are shown in Tables VII and IX. The ε_1 phase was found to be a 7 layer structure and the ε_3 phase a 6 layer one.

To determine the possible layer stacking in the new Laves phase ε_1, Kamura's analysis was used. Using the layer sequence shown in Fig. 8, all the 7 layer sequences were written out. This turns out to be 64 in number. Of these, only a few are possible. The possible sequences are determined with the help of the following two facts:

(i) if the sequence started with layer A, the eight layer must again be an A layer. Those sequences, having the eighth layer not the same as the first layer were discarded.

(ii) if any sequence starting with layer A resembled those of another sequence when the layers were counted from some where in the middle, the two sequences were the same and to be counted only once.

Using these criteria the total number of sequences reduced to 17 with A followed by B and A followed by B' sequences. These sequences are shown in Table XIII. Intensity calculations on the basis of these possible sequences has been started to determine which sequence out of the possible 17 is the most probable one. So far only

5 sequences (No. 1 to 5) have been tried. None of these appear to give correct intensity relationships that is desired. Further work will be necessary to identify the correct stacking sequence.

CONCLUSION

1. μ phase extends from the binary in the Mo-(Fe,Co)-Si systems and a very small ternary μ phase region appears around 10 at pct Si in the Mo-Ni-Si system.
2. μ phase region extends along a constant Mo line in the Mo-Co-Si system but extends in two directions one along a constant Mo and the other along increasing Mo in the Mo-Fe-Si system.
3. The extension of the μ phase region from the binaries and the stabilization of a ternary μ phase appear to be guided by both electronic factor (e/a) and size factor.
4. Ternary R phases have been found in the Mo-Co-Si and Mo-Ni-Si systems, very close to the μ phase region.
5. Six new Laves type phases related to the $MgZn_2$ type Laves phases have been discovered. All theses phases are rather narrow and extend along the 33.3 at pct Mo line.
6. Mo-Fe-Si and Mo-Co-Si have one of the Laves type phase (ε_1) common. The ε_1 phase is hexogonal with seven Komura layers.
7. The ε_3 phase in the Mo-Fe-Si appears to be a six Komura layer Laves phase.

REFERENCES

1. M.V. Nevitt ''Electronic Structure and Alloy Chemistry of the Transition Elements'', P.A. Beek ed. John Wiley and Sons New York, 1963.
2. R.M. Waterstrat, Trans. AIME 221 (1961) 687.
3. D.S. Bloom and N.J. Grank, Trans. AIME 197 (1953) 88
4. Peter Greenfield and P.A. Beck:
   ''The σ phase in binary alloys''
   Trans. AIME 253 (1954) 200.
5. S.K. Gupta and K.P. Gupta:
   ''Phase equilibria at the high Mn end of the Mn-Ti-V and Mn-Ti-Cr system''
   Trans. I.I.M. 29 (1976) 859.
6. F.C. Frank and J.S. Kesper:
   Acta Cryst. 11 (1958) 184.
7. J.S. Kasper ''Theory of alloy phases''
   ASM Cleveland Ohio (1956).
8. P.C. Panigrahy and K.P. Gupta:
   Trans. TSM-AIME 245 (1969) 1533.
9. W.D. Manly, E.L. Kaman and S.P. Ridesut and P.A. Beek:
   ''Intermediate phases in ternary alloy systems of

Transition elements"
Trans AIME 191 (1951) 872.

10. B.N. Das and P.A. Beck "Relationship between the and phases in the Mo-Mn-Co system"
Trans AIME 218 (1960) 733.

11. A.G.H. Anderson and E.R. Jetti, "X-ray investigation of Fe-Cr-Si phase diagram"
Trans. ASM 24 (1936) 375, and B. Aronsson and T. Lundstram 'Investigation on Fe-Cr-Si" Acta Chemica Scandinavia 11 (1957) 365.

12. K.P. Gupta, N.S.S. Rajan and P.A. Beek:
"Effect of Si and Al on the stability of certain phases"
Trans. AIME 218 (1960) 617.

13. D.I. Bardos, K.P. Gupta and P.A. Beek:
"New Ternary R-phase with Si" Nature 192 (1961) 144.

14. D.I. Bardos and K.P. Gupta and P.A. Beek:
"Ternary Laves phases with Transition elements with Si" Trans. AIME 221 (1961) 1087.

15. Y.B. Kuzma and E.I. Gledyshevskii:
J. of Structural Chemistry 1 (1960) 57.

16. A. Raman: Z. Metallkde 60 (1969) 57.

17. A.K. Jena and K.P. Gupta "Phase Stability"
Procedings of the Silver Jubilee Symposium I.I.M. 1972.

18. M. Henson "Constitution of Binary Alloys"
Mc.Graw Hill Book. Co. New York 1958.

19. D.K. Das, S.P. Redcout and P.A. Beek:
J. Metals 1952.

20. C.B. Shoemaker, D.P. Shoemaker and J. Moller
"Neutron Diffraction studies of the order of the atoms in the P and R phase".
Acta Cryst. 18 (1965) 37.

21. T. Yoshioka and P.A. Beek. "The Atomic Volume of Si, Ge and Ti" Trans. Met. Soc. AIME 233 (1965) 1788.

22. B.N. Singh and K.P. Gupta: Metallurgical Trans. 1 (1970).

23. F. Laves in "Theory of Alloy Phases" ASM Cleveland Ohio (1956).

24. Y. Komura "Stacking Faults and Two New Modification of the Laves phase in Mg Cu Al system" Acta Cryst. 15 (1962) 770.

25. Y. Komura, M. Metaria, I Nakatani H. Eba & T. Shimizls.
"Structural changes in the alloy system Mg-Zr-Cu and Mg Zn-Ag" Acta crystallographic.

TABLE I

Crystallographic Data, Radious Ratio, and Electron:Atom Ratio for some Transition Metal complex phases*.

S.No.	Phase	Space Group	No.ofatoms per cell	CN of Different Crystallographic sites	RA/RB	/a
1	σ	D_{4h}^{14}-P_{42}/mnm	30	CN12, CN14, CN15	0.93-1.15	5.6- 7.6
2	P	D_{2h}^{16}-Pbnm	56	CN12, CN14, CN15,CN16	1.09-1.11	7.15-7.76
3	R	C_{zi}^{2}-$R_{\bar{3}}$	53	CN12, Cn14, CN15,CN16	1.05-1.12	6.43-7.54
4	μ	D_{3}^{5} - R_{3m}	13	CN12, CN14, CN15, CN16	1.10-1.18	7.08-7.62
5	×(α-Mn)	T^{3} - $I4^{3m}$	58	CN12, CN13, CN16	1.02-1.21	6.24-7.24
6	β -Mn	O^{6} - P_{43}^{32}	20	CN12(I), CN12(II)	-	6.85-7.8
7	Laves phase	Oh^{7}-Fd 3m D_{6h}^{4}-$P6_3/mne$	24 12	CN12, CN16	1.05-1.68	1.83+2.32
8	Cr_3O	O_h^3 - Pm_3n	8	CN14, CN12	.810-1.111	-

* References are given in the reference Table.

TABLE II

Phase analysis of the Mo-Fe-Si system

Alloy No.	Intended Composition of alloy in At pct. of			No. of phases present	Phase identification by Xray analysis
	Mo	Fe	Si		
1	50.0	45.0	5.0	3	$\sigma + \mu$
2	45.0	50.0	5. 0	2	μ
3	40.0	55.0	5.0	2	μ
4	35.0	60.0	5.0	2	μ
5	50.0	40.0	10.0	2	μ+B.C.C.
6	44.0	46.0	10.0	2	$\mu+\varepsilon_1$
7	40.0	50.0	10.0	2	$\mu+\varepsilon_1$
8	35.0	55.0	10.0	2	ε_1
9	43.0	55.0	2.0	1	μ
10	60.0	30.0	10.0	2	μ+B.C.C.
11	55.0	35.0	10.0	2	μ+B.C.C.
12	47.0	43.0	10.0	2	$\mu+\varepsilon_1$
13	44.0	41.0	15.0	3	ε_1+ B.C.C.
14	47.0	48.0	5.0	1	μ
15	30.0	65.0	5.0	2	μ+f.c.c.
16	32.5	55.0	12.5	2	ε_1
17	35.0	50.0	15.0	2	ε_1
18	25.0	60.0	15.0	2	ε_1
19	49.0	50.0	2.0	2	$\sigma+\mu$

Table II Contd.

Alloy No.	Intended Composition of alloy in At pct. of			No. of pheses present	Phase identification by X-ray analysis
	Mo	Fe	Si		
20	38.0	57.0	5.0	1	μ
21	35.0	45.0	20.0	2	ε_2
22	35.0	40.0	25.0	2	ε_3
23	35.0	35.0	30.0	2	ε_3
24	49.0	44.5	6.5	3	$\mu+\varepsilon_1$+b.c.c.
25	37.5	55.5	7.0	1	μ
26	35.0	52.5	12.5	2	$\varepsilon_1+\mu$
27	35.0	47.5	17.5	2	ε_2
28	35.0	42.5	22.5	2	ε_2
29	35.0	32.0	33.0	2	ε_3
30	35.0	30.0	35.0	3	ε_3
31	40.0	58.0	2.0	1	μ
32	41.0	52.0	7.0	2	μ
33	33.0	35.0	17.0	3	$\varepsilon_2+\varepsilon_1$
34	33.0	44.0	23.0	1	ε_1
35	33.0	32.0	35.0	2	ε_3
36	38.0	54.0	8.0	2	μ
37	33.0	41.0	26.0	1	ε_3

TABLE III

Phase analysis of the Mo-Fe-Si system

Alloy No.	Intended Composition of alloy in at pct of			No. of phases present	Phase identification by X-ray analysis
	Mo	Co	Si		
1	50.0	45.0	5.0	3	$\mu+\sigma$
2	45.0	50.0	5.0	2	μ
3	40.0	55.0	5.0	2	μ+f.c.c
4	35.0	60.0	5.0	2	μ+f.c.c
5	40.0	50.0	10.0	2	$\mu+\varepsilon_1$
6	50.0	40.0	10.0	2	μ+B.C.C.
7	45.0	45.0	10.0	2	$\mu+\varepsilon_1$
8	60.0	35.0	5.0	2	$\mu+\sigma$+ B.C.C.
9	55.0	40.0	5.0	2	μ+B.C.C.
10	55.0	35.0	10.0	2	ε_1
11	35.0	52.0	13.0	2	$\varepsilon_1+\mu$
12	43.0	42.0	15.0	2	$\varepsilon_1+\mu$
13	37.0	47.0	16.0	2	ε_1
14	31.0	53.0	16.0	2	ε_1
15	32.0	48.0	20.0	1	ε_1
16	33.0	55.0	12.0	2	ε_1
17	35.0	45.0	20.0	2	ε_1
18	31.0	49.0	20.0	2	ε_1
19	33.0	34.0	23.0	2	

Table III Contd.

Alloy No.	Intended Composition of alloy in at pct of			No. of Phases present	Phase identification by X-ray analysis
	Mo	Co	Si		
20	49.0	36.0	15.0	2	μ
21	47.0	39.0	15.0	2	μ
22	47.5	34.5	18.0	2	μ
23	33.0	59.0	8.0	3	μ
24	20.0	75.0	5.0	2	$\mu+\varepsilon_1$+B.C.C.
25	25.0	65.0	10.0	2	μ+f.c.c.
26	49.0	33.0	18.0	2	μ
27	48.0	32.0	20.0	3	R
28	46.0	36.0	18.0	2	μ
29	33.0	34.0	33.0	2	ε_4
30	33.0	37.0	30.0	1	ε_4
31	32.0	40.0	28.0	2	ε_4
32	34.0	41.0	25.0	2	ε_4
33	47.0	32.0	21.0	3	R+μ
34	34.0	31.0	35.0	2	ε_4
35	45.0	32.0	23.0	3	R+$\mu+\varepsilon_4$
36	44.0	32.0	24.0	3	R+$\mu+\varepsilon_4$
37	49.0	27.0	24.0	2	R
38	49.0	29.0	22.0	2	R
39	45.5	34.5	20.0	3	μ+ R

TABLE IV

Phase analysis of the Mo-Ni-Si system

Alloy No.	Intended Composition of alloy in at pct of			No. of phases present	Phase identification by X-ray analysis
	Mo	Ni	Si		
1	50.0	40.0	5.0	1	R
2	45.0	50.0	5.0	3	R+f.c.c.
3	40.0	55.0	5.0	3	R+ε_1+ f.c.c.
4	35.0	60.0	5.0	3	R+ε_1+f.c.c.
5	30.0	65.0	5.0	3	R+ε_5+f.c.c.
6	60.0	30.0	10.0	2	R+ B.C.C.
7	50.0	40.0	10.0	2	μ
8	40.0	50.0	10.0	3	ε_5+ R
9	30.0	60.0	10.0	3	ε_5+ f.c.c.
10	45.0	40.0	15.0	3	R +ε_6
11	35.0	50.0	15.0	3	ε_5+μ
12	53.0	47.0	-	2	δ
13	55.0	40.0	5.0	3	R + B.C.C.
14	55.0	35.0	10.0	3	R+ε_6+ B.C.C.
15	63.0	25.0	12.0	3	R+ε_6+ B.C.C.
16	55.0	30.0	15.0	3	R+ε_6+ B.C.C.
17	50.0	30.0	15.0	3	R+ε_6+ B.C.C.
18	40.0	45.0	15.0	3	μ+ε_6+ R
19	30.0	55.0	15.0	2	μ_5

Table IV contd.

Alloy No.	Intended Composition of alloy in at pct of			No. of phases present	Phase identification by X-ray analysis
	Mo	Ni	Si		
20	25.0	60.15	15.0	2	ε_5 + B.C.C.
21	30.0	50.0	20.0	2	ε_5
22	25.0	55.0	20.0	2	ε_5
23	53.0	45.0	2.0	2	δ + B.C.C.
24	59.50	41.50	5.0	3	R + B.C.C.
25	51.5	43.50	5.0	3	R+δ
26	52.5	37.50	10.0	3	R
27	32.0	54.0	14.0	3	ε_5
28	34.0	46.0	20.0	3	ε_5 + ε_6
29	32.0	46.0	22.0	3	ε_5 + ε_6
30	48.0	38.0	14.0	2	ε_6
31	33.0	43.0	24.0	3	ε_6 + R
32	32.0	38.0	30.0	1	ε_6
33	51.5	39.5	9.0	3	R + μ
34	32.0	33.0	35.0	3	ε_6
35	30.0	40.0	30.0	2	ε_6
36	31.0	30.0	39.0	2	ε_6
37	51.0	40.0	9.0	2	μ+R
38	32.0	47.50	20.5	2	ε_5 + ε_6
39	32.50	50.50	17.50	1	ε_5
40	50.0	41.0	9.0	3	R + μ

TABLE V

X-ray diffraction pattern of μ phase in the ternary system Mo-Fe-Si and Mo-Co-Si.

Diffraction pattern of alloy 20 of (Mo-Fe-Si) ao=4.762 Co=25.615 C/a=5.379				Diffraction pattern of alloy 21 of (Mo-Co-Si) ao= 4.8450 Co=26.930 C/a = 5.600			
S.No.	R.I	d observed	d calculated	hxl	RI	d observed	d calculated
1	-	-	-	016	VW	3.0735	3.0652
2	-	-	-	017	VW	2.7924	2.8357
3	M	2.5909	2.5733	108	VW	2.6105	2.6105
4	-	-	-	0.0,11	VW	2.5335	2.4482
5	VS	2.3595	2.7592	110	VS	2.3728	2.4227
6	M	2.2819	2.2793	113	W	2.2860	2.3390
7	VW	2.2182	2.2135	1,0,10	-	-	-
8	VW	2.1926	2.2085	00,12	VW	2.2224	2.2444
9	S	2.1723	2.1552	115	S	2.1874	2.2094
10	M	2.1053	2.0808	116	VW	2.1462	2.1319
11	VS	2.0689	2.0754	1,0,11	M	2.0969	2.0981
12	M	2.0445	2.0431	200	-	-	-
13	S	2.02214	2.0193	202	VS	2.0774	2.073
14	W	1.9515	1.9525	204	S	2.0410	2.0031
15	S	1.9064	1.9063	205	M	1.1956	2.9550
16	W	1.8412	1.8412	119	M	1.9098	1.8829
17	VW	1.8131	1.8242	1,0,13	W	1.8315	1.8575
18	-	-	-	0,0,15	W	1.7925	1.7954

Table V contd.

S.No.	R.I	d observed	d calculated	hxl	R.I	d observed	d calculate
19	-	-	-	208	W	1.7612	1.7806
20	VW	1.4436	1.4430	0,2,13	-	-	-
21	-	-	-	00,18	VW	1.4961	1.4961
22	VW	1.42779	1.4299	1,2,7	VW	1.4600	1.4663
23	VW	1.4144	1.4142	1,1,15	-	-	-
24	VW	1.3832	1.3852	10,18	-	-	-
25	VVS	1.3676	1.3677	129	-	-	-
26	-	-	-	20,14	VW	1.4210	1.4179
27	VW	1.3637	1.3620	3 0 0	VW	1.3932	1.3987
28	VS	1.3309	1.3341	3 0 4	VS	1.3695	1.3695
29	VS	1.3064	1.3015	306	VS	1.3311	1.3354
30	VS	1.2964	1.3062	21,11	VS	1.3047	1.3311
31	-	-	-	20,16	S	1.2958	1.3129
32	M	1.2679	1.2656	12,12	S	1.2835	1.2824
33	-	-	-	11,18	S	1.2692	1.2730
34	W	1.2336	1.2336	309	S	1.2580	1.2670
35	VS	1.2266	1.2310	12,13	S	1.2281	1.2593
36	-	-	-	2,1,14	S	1.2224	1.2237
37	M	1.2205	1.2114	30,10	-	-	-
38	VS	1.1892	1.1856	03,11	-	-	-

Table V contd.

S.No.	R.I.	$d_{observed}$	$d_{calculated}$	hxl	R.I	$d_{observed}$	$d_{calculated}$
39	-	-	-	223	VW	1.19880	1.2004
40	-	-	-	12,15	VS	1.1873	1.1886
41	-	-	-	3,0,12	S	1.1852	1.1870

NOTE:-

Key to symbols used in Tables:

VVW	:	Very very weak	S	:	Strong
VW	:	Very weak	VS	:	Very strong
W	:	Weak	VVS	:	Very very strong
M	:	Medium			

TABLE VI

X-ray diffraction pattern of ε_1 phase in the ternary systems

Mo-Fe-Si & Mo-Co-Si

Diffraction pattern of alloy (8) of Mo-Fe-Si				Diffraction pattern of alloy (15) of Mo-Co-Si		
ao=4.748 Co=27.040229 c/a=5.69				ao=4.8566 Co=27.9600		C/a=5.757
RI	d observed	d calculated	hkl	d observed	d calculated	R.I
-	-	-	102	4.045	4.0194	VW
-	-	-	104	3.5465	3.5805	VW
-	-	-	105	3.2470	3.3318	VW
-	-	-	009	3.0357	3.0329	VW
-	-	-	0,0,10	2.7744	2.7296	VW
VW	2.57464	β	—	-	-	-
VW	2.45709	2.45709	0,0,11	2.5784	2.4815	W
VW	2.3806	2.3744	110	-	-	-
VS	2.34315	2.3386	112	3.3500	3.3908	S
W	2.2552	2.2534	0,0,12	-	-	-
VW	2.2028	-	-	2.3065	-	-
VS	2.1623	2.1747	115	2.2547	2.2187	VS
S	2.1236	2.1100	10,11	2.1945	2.1372	S
S	2.0617	2.0563	200	2.1544	2.1030	VS
VW	2.0402	2.0329	022	-	-	-
VS	2.0193	2.0228	117	2.1218	2.0613	S

Table VI contd.

R.I	d observed	d calculated	hkl	d observed	d calculated	R.I
S	1.9717	1.9762	10,12	2.033	-	S
VW	1.92116	1.9220	024	2.000	2.0008	VS
VW	1.92116	1.9220	205	1.9655	1.9624	VS
VW	1.8954	1.8708	206	1.9030	1.9089	W
	-	-	208	1.7989	1.7902	W
	-	-	209	1.7222	1.7282	W
	-	-	-	1.5546	-	VW
W	1.5273	1.5318	213	1.5302	1.5442	
W	1.45896	1.4623	2013	1.5080	1.5007	W
W	1.4436	1.4420	127	1.4891		W
VW	1.4154	1.4122	128	1.4457		M
VS	1.3682	1.3691	031	1.4266		S
S	1.3558	1.3555	2015	1.4053	1.4080	M
VVW	1.3425	1.3449	00,19	-	-	-
VS	1.3285	1.3288	305	1.3578	1.3579	VS
VS	1.3083	1.3115	306	1.3408	1.3398	M
VS	1.30204	1.3056	2016	1.3173		
VVW	1.2935	1.2919	037	-	-	-
VS	1.28763	1.2876	0021	1.2998	1.2998	S
VW	1.2822	1.2795	21,12	-	-	-

Table VI contd.

R.I	d observed	d calculated	hkl	d observed	d calculated	R.I
-	-	-	308	1,2926	1.2968	M
-	-	-	2,0,17	1,2798	1.2762	S
-	-	-	309	1.2718	1.2726	W
VW	1.2671	1.2695	1,1,18	-	-	-
VS	1.2355	1.2291	0,0,22	-	-	-
W	1.2247	1.2227	0,3,10	-	-	-
W	1.21816	1.2207	1,1,19	1.2220	1.2206	W
	-	-	220	1.219	1.2142	S
	-	-	221	1.2137	1.2130	M
W	1.20953	1.2110	2,1,14	-	-	-
	-	-	223	1.1995	1.2035	M
	-	-	1,2,15	1.1974	1.1172	W
	-	-	1,0,22	1.1912	1.1900	W
S	1.872	1.1872	220	-	-	-
	-	-	225	1.18503	1.1852	W
	-	-	226	1.1781	1.1731	S
	-	-	310	1.1758	1.1665	M

TABLE VII

X-ray diffraction pattern of ε_2 of (Mo Fe Si)-Alloy No.21

Line No.	R.I	d calculated
1	VW	2.6105
2	W	2.3993
3	S	2.3688
4	W	2.1234
5	VS	2.1793
6	W	2.1310
7	VW	2.0811
8	VW	2.0485
9	VS	2.01967
10	S	1.9844
11	VW	1.9530
12	VW	1.90708
13	VW	1.7289
14	W	1.4558
15	W	1.4400
16	W	1.4130
17	M	1.3654
18	M	1.3520
19	VS	1.3274

Table VII contd.

Line No.	R.I.	d calculated
20	M	1.3048
21	S	1.2896
22	VS	1.2335
23	VW	1.2259
24	VW	1.2091
25	S	1.18643
26	M	1.184379

TABLE VIII

X-ray diffraction pattern of ε_3 phase alloy No. 23 of Mo-Fe-Si system

ao = 4.854 Co = 22.971 c/a = 4.735

S.No.	R.I.	hkl	d observed	d calculated
1	VW	101	4.0918	4.1349
2	VW	103	3.6182	3.6848
3	VW	104	3.3698	3.392
4	VW	105	3.0583	3.1013
5	W	106	2.7948	2.8305
6	W	009	2.6997	2.5523
7	M	line	2.60210	-
8	W	110	2.50774	2.4269
9	VS	108	2.3684	2.3710
10	VW	113	2.3349	2.3135
11	VW	00,11	2.0963	2.2971
12	S	-	2.2474	-
13	S	114	2.2943	2.355
14	VS	109	1.1626	2.1817
15	VW	115	2.1445	2.1459
16	S	200	2.10208	2.10207
17	S	116	2.0508	2.0498
18	VS	1,0,10	2.0140	2.0148

Table VIII contd.

S.No.	R.I.	hkl	d observed	d calculated
19	VS	204	1.9813	1.9737
20	W	117	1.9357	1.9513
21	W	0,0,12	1.9140	1.9142
22	W	208	1.7180	1.6960
23	VW	2,0,10	1.5411	1.5506
24	M	126	1.4604	1.4675
25	M	1,0,15	1.4386	1.4389
26	M	2,0,12	1.4193	1.4152
27	S	303	1.3709	1.3783
28	W	0,0,17	1.3512	1.3512
29	VS	306	1.3289	1.3158
30	M	1,2,10	1.3061	1.3067
31	VS	20,14	1.2923	1.2933
32	W	0,0,18	1.2781	1.2762
33	W	2,1,11	1.2661	1.2644
34	VS	1,1,16	1.2304	1.2357
35	S	039	1.2283	1.2283
36	W	1,2,12	1.2229	1.2226
37	M	0,0,19	1.2082	1.2090
38	W	223	1.1967	1.1985
39	VW	03,10	1.9324	1.1962
40	VS	224	1.8849	1.1872

TABLE IX

X-ray diffraction pattern of ε_4 phase of alloy No. 30 of Mo-Co-Si system.

Line No.	R.I.	d calculated
1	VW	2.8183
2	M	2.5852
3	S	2.3703
4	VW	2.2527
5	M	2.2069
6	M	2.1769
7	S	2.1450
8	M	2.0542
9	VS	2.0071
10	VS	1.9821
11	W	1.8839
12	W	1.4509
13	W	1.4306
14	W	1.41392
15	M	1.40857
16	M	1.33410
17	VS	1.31708
18	M	1.30111
19	S	1.28614

Table IX contd.

Line No.	R.I.	d calculated
20	M	1.2585
21	S	1.2164
22	M	1.21408
23	W	1.20212
24	W	1.9892
25	W	1.9666
26	VW	1.8884
27	VS	1.8554
28	S	1.1835
29	W	1.7821

TABLE X

X-ray diffraction pattern of ε_5 phase of alloy number (39) of Mo-Ni-Si system

S.No.	R.I.	d observed
1	W	2.57865
2	S	2.3414
3	M	2.1890
4	VS	2.1538
5	M	2.0885
6	M	2.0292
7	VS	1.9972
8	VS	1.9606
9	VW	1.9008
10	VW	1.7981
11	W	1.4501
12	W	1.4299
13	W	1.4089
14	M	1.3598
15	M	1.3424
16	S	1.3182
17	M	1.2910
18	S	1.2800
19	S	1.2232

Table X contd.

S.No.	R.I.	d observed
20	W	1.2165
21	M	1.19826
22	W	1.19093
23	W	1.1863
24	S	1.1775
25	M	1.1753

Table XI

X-ray diffraction pattern of ε_6 phase of alloy No. 32 of Mo-Ni-Si

S.No.	R.I.	d observed
1	VW	2.7696
2	VW	2.5908
3	VS	2.3568
4	M	2.2544
5	M	2.2022
6	M	2.1634
7	VS	2.1438
8	W	2.1189
9	S	2.0508
10	VS	2.0168
11	VS	1.9780
12	W	1.8903
13	VW	1.4514
14	VW	1.4344
15	VW	1.4204
16	VW	1.4114
17	M	1.3674
18	M	1.3373
19	VS	1.3214

Table XI contd.

S.No.	R.I.	d observed
20	M	1.30213
21	S	1.2877
22	M	1.2837
23	W	1.2618
24	VS	1.2188
25	S	1.2166
26	W	1.2070
27	M	1.2004
28	VW	1.1984
29	VW	1.1906
30	VS	1.1850
31	S	1.1832

TABLE XII

X-ray diffraction Pattern of R-phase, alloy No.(38) of Mo-Co-Si system

a_o = 11.0389 Co = 19.684 C/a = 1.778

S.No.	R.I.	hkl.	d observed	d calculated
1	M	126	2.4388	2.4289
2	M	041,134	2.3538	2.3342
3	M	306	2.2840	2.2840
4	VS	217	2.2156	2.2192
5	VS	230	2.1949	2.1932
6	S	232	2.1399	2.1407
7	S	140	2.0867	2.0862
8	VW	142	2.0413	2.0408
9	W	128	2.0341	2.0338
10	W	234	2.0031	2.0031
11	VW	209	1.9887	1.9888
12	W	317	1.9286	1.9291
13	W	502	1.8744	1.8744
14	W	240	1.8064	1.8064
15	W	2013	1.4434	1.4435
16	W	4,1,10	1.4305	1.4305
17	W	256	1.3896	1.3896
18	W	441	1.3773	1.3772
19	W	1,1,14	1.3634	1.3634

Table XII contd.

S.No.	R.I.	hkl	d observed	d calculated
20	M	261	1.3200	1.3227
21	VS	1,2,14,0,0,15	1.3111	1.3103
22	S	355;075	1.2914	1.2903
23	S	170	1.2681	1.2681
24	S	172	1.2558	1.2559
25	S	2,3,13	1.2461	1.2461
26	M	262	1.2296	1.2296
27	M	450	1.2234	1.2240

TABLE XIII

1	A	B	C	A	B	C'	B'	A
2	A	B	C	A	B'	A	B'	A
3	A	B	C	A	B'	A'	C	A
4	A	B	C	A'	C	A	B'	A
5	A	B	C	A'	C	A'	C	A
6	A	B	C	A'	C'	B	C	A
7	A	B	C	B	C	A	B'	A
8	A	B	C	B	C	A'	C	A
9	A	B	C'	B	C'	B	C	A
10	A	B	C'	B'	A	B	C	A
11	A	B	C'	B'	A'	C'	B'	A
12	A	B'	A	B'	A'	C'	B'	A
13	A	B'	A'	C'	B'	A'	C	A
14	A	B'	A'	C'	B'	A	B'	A
15	A	B'	A'	C'	B	C'	B'	A
16	A	B'	A'	C	A'	C'	B'	A
17	A	B'	A'	C	A'	C	B'	A

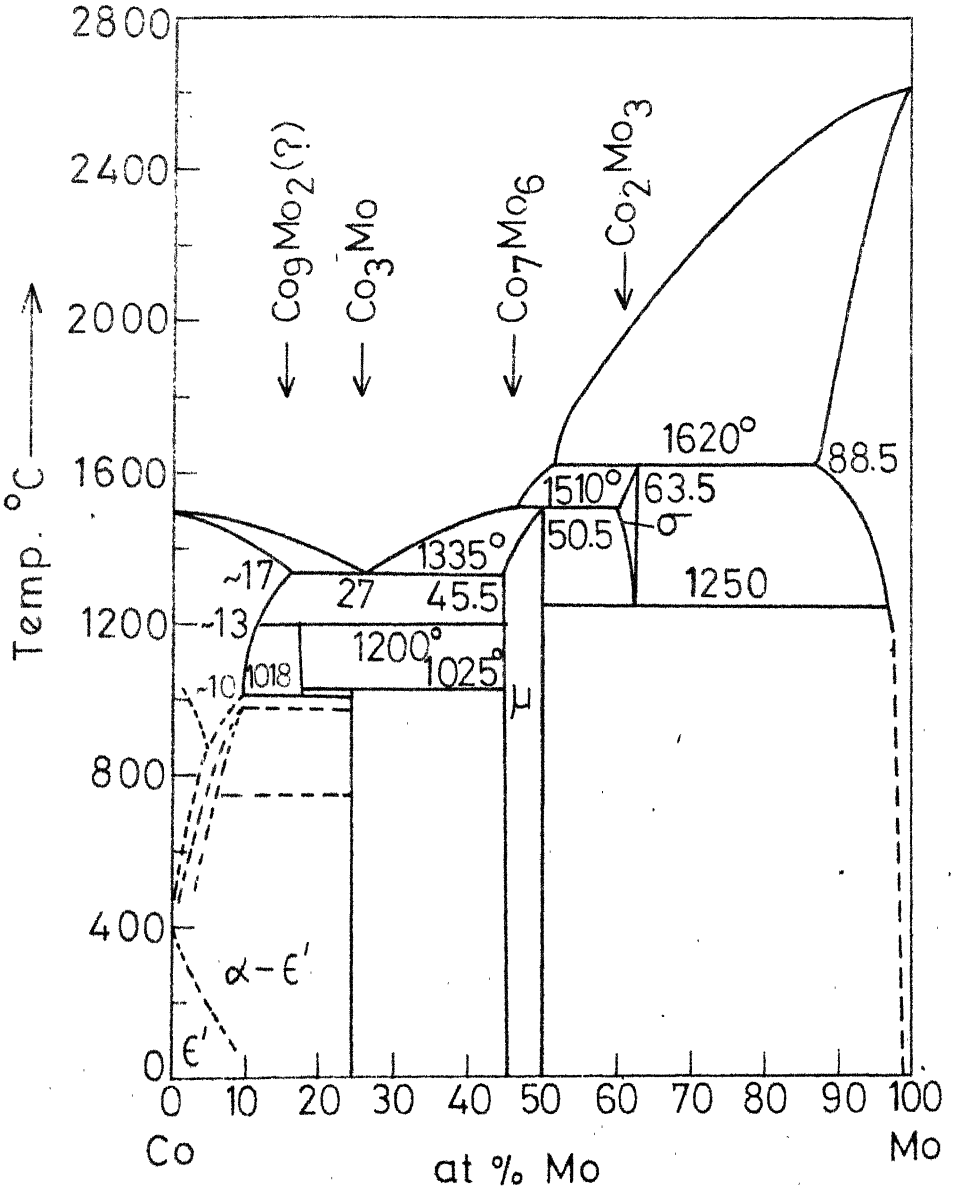

FIG.1 Co-Mo PHASE DIAGRAM
(reproduced from ref 18)

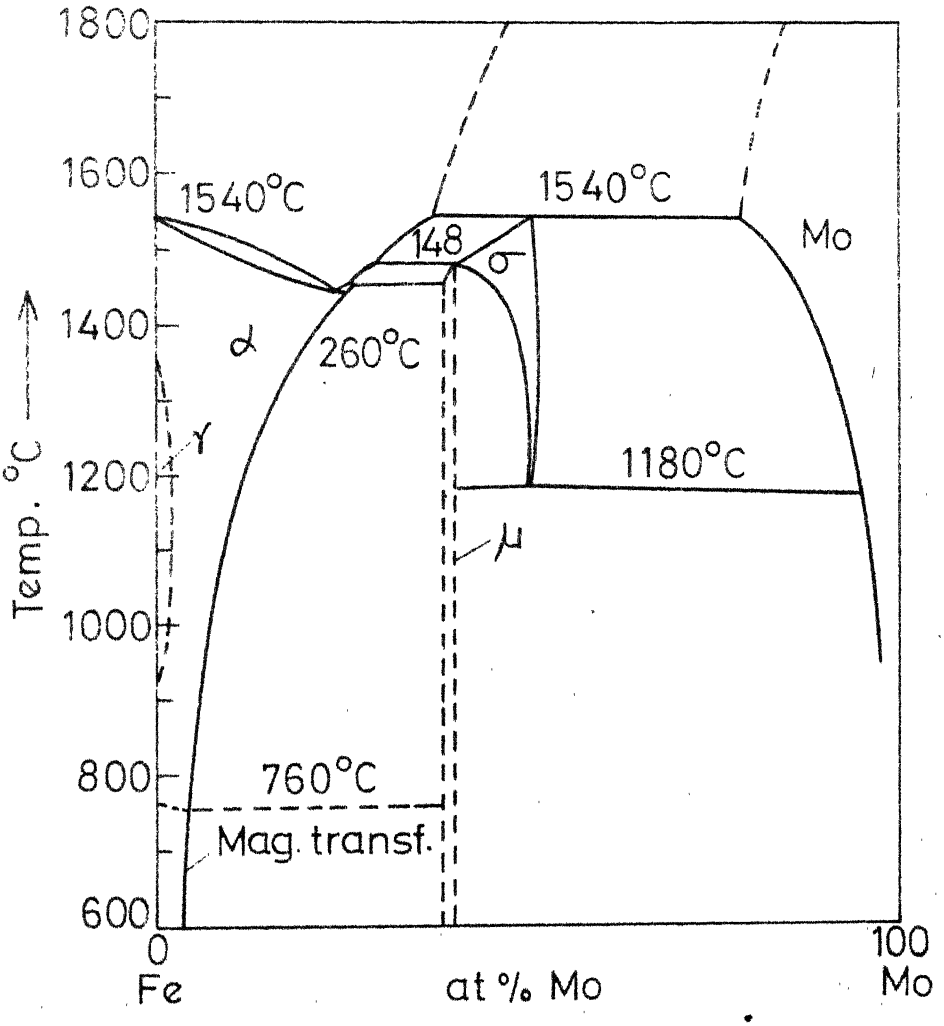

FIG. 2 Fe – Mo PHASE DIAGRAM
(reproduced from ref 18)

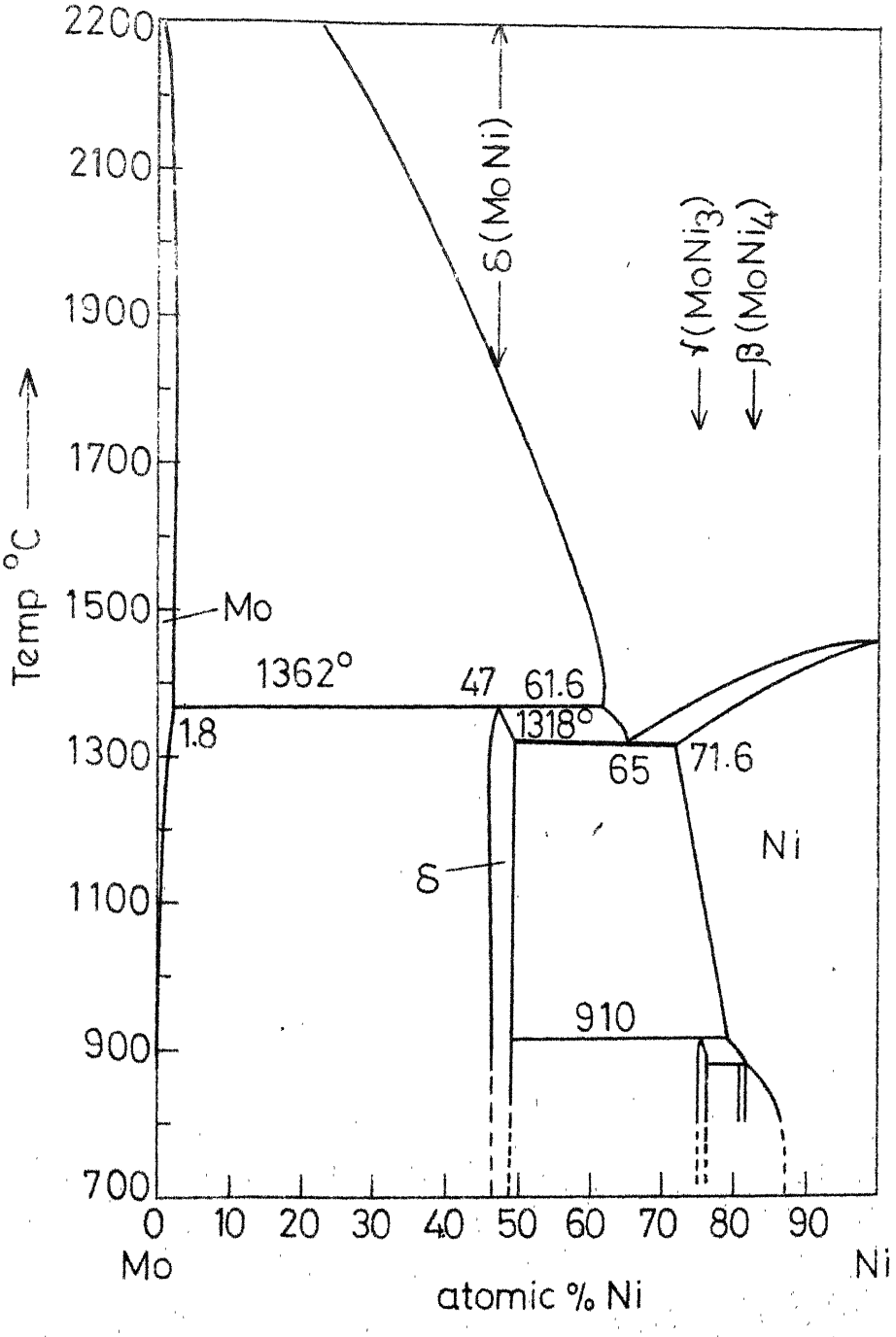

FIG. 3 Mo-Ni PHASE DIAGRAM
(reproduced from ref 18)

ISOTHERMAL SECTION OF Mo-Co-Si SYSTEM AT 1280°C

FIG. 4

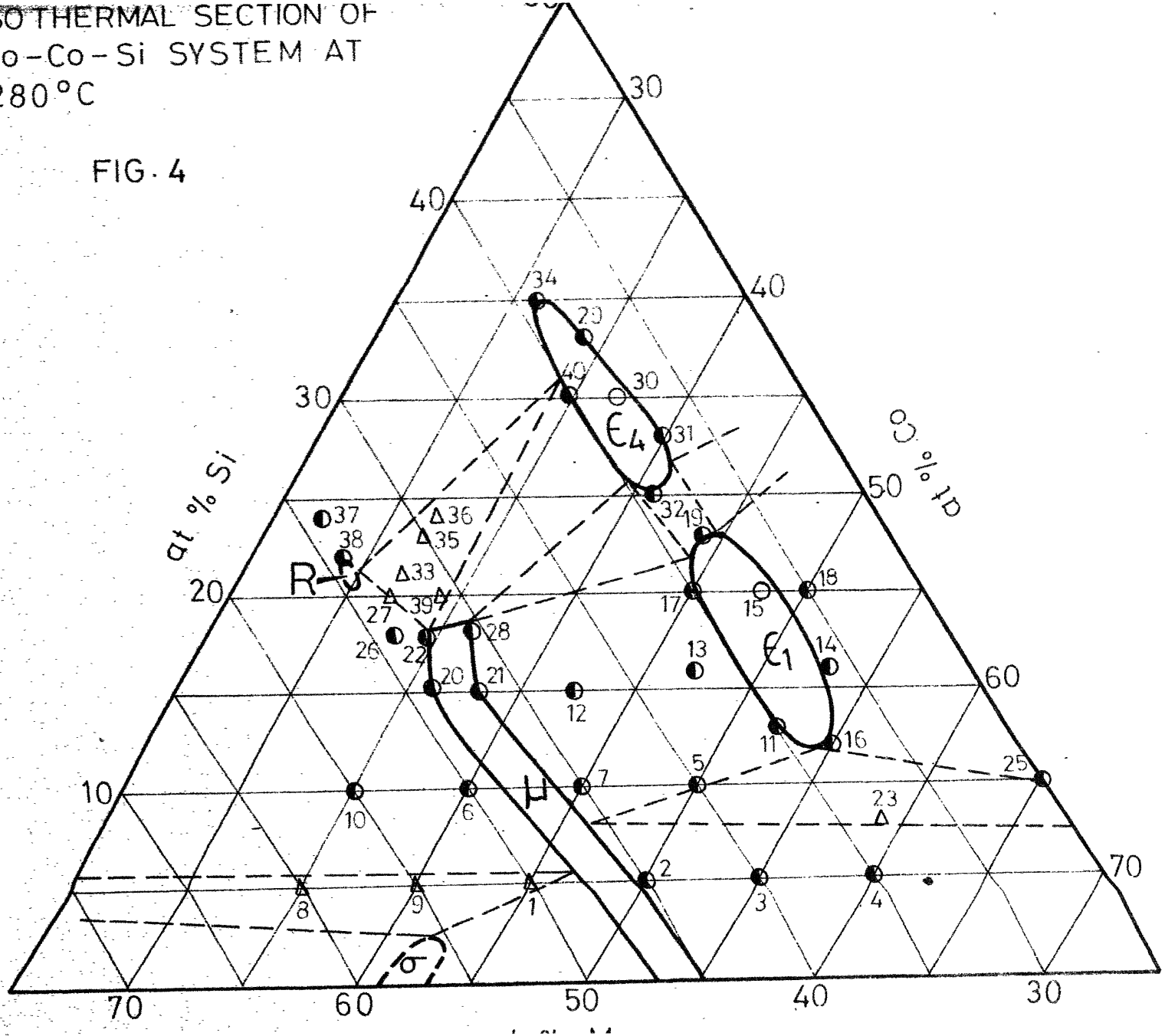

ISOTHERMAL SECTION OF
Mo-Fe-Si SYSTEM AT
1280°C

FIG. 5

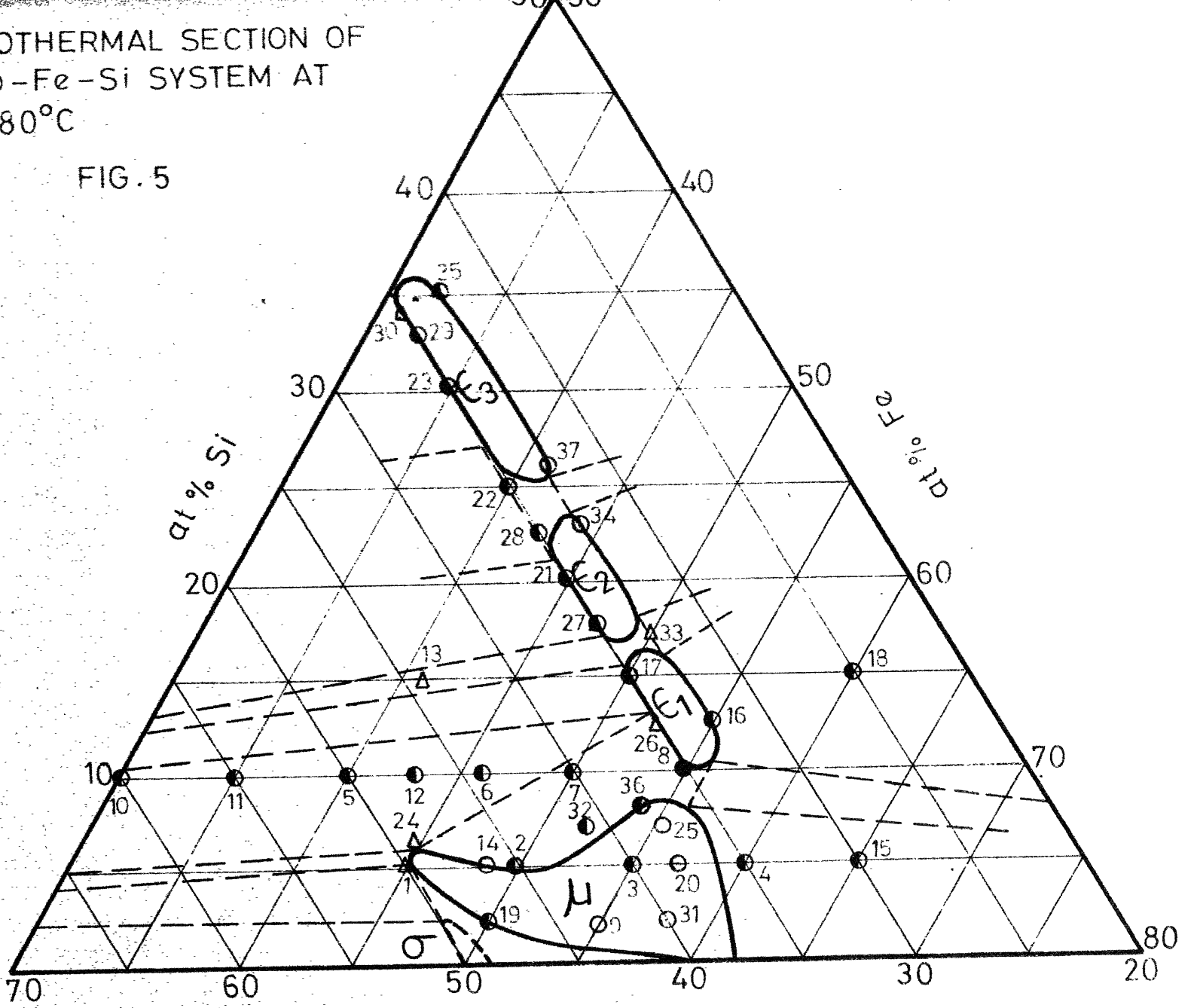

ISOTHERMAL SECTION OF
Mo - Ni - Si SYSTEM AT
1280 °C

FIG. 6

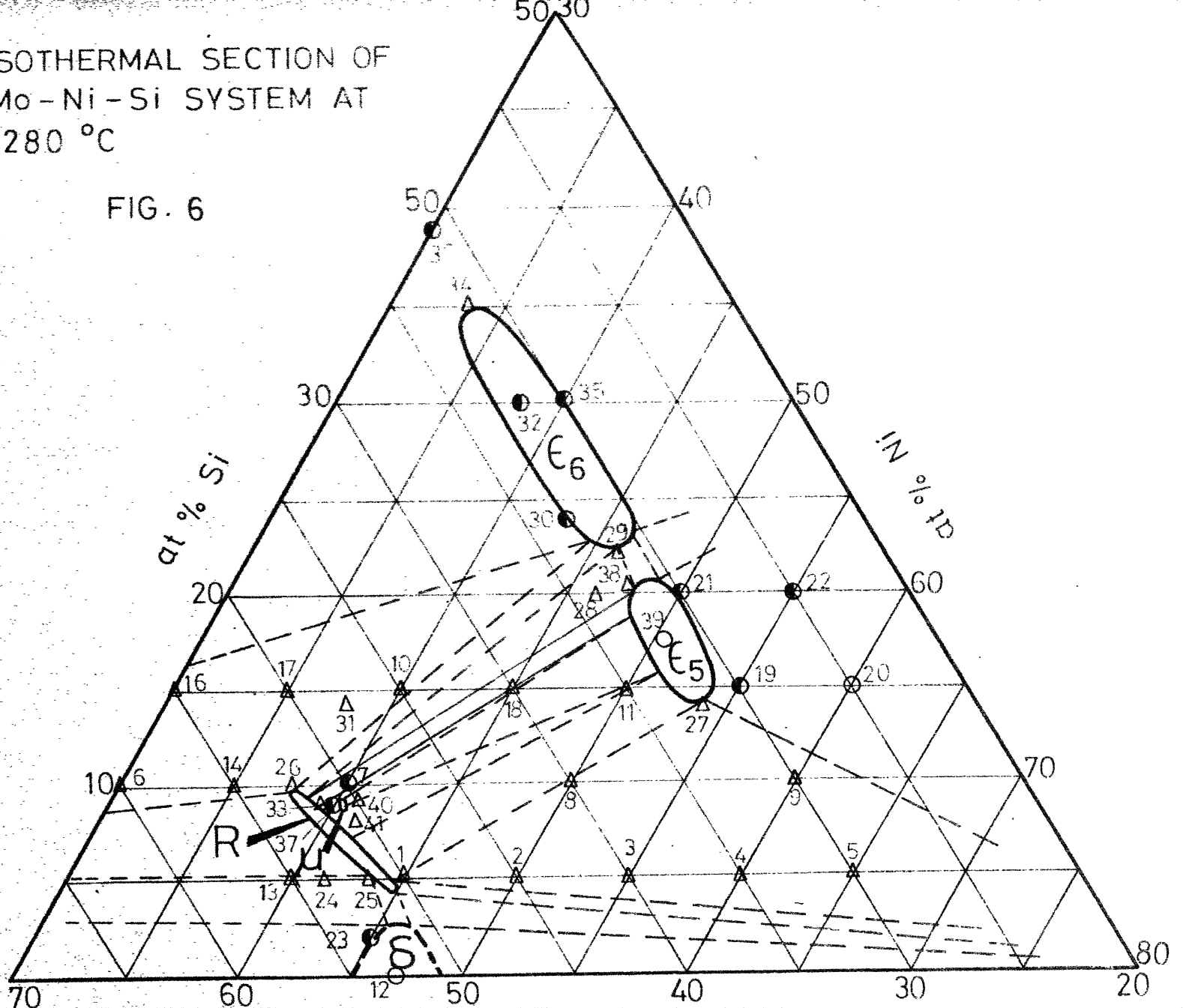

Fig. 7 Six fundamental layers

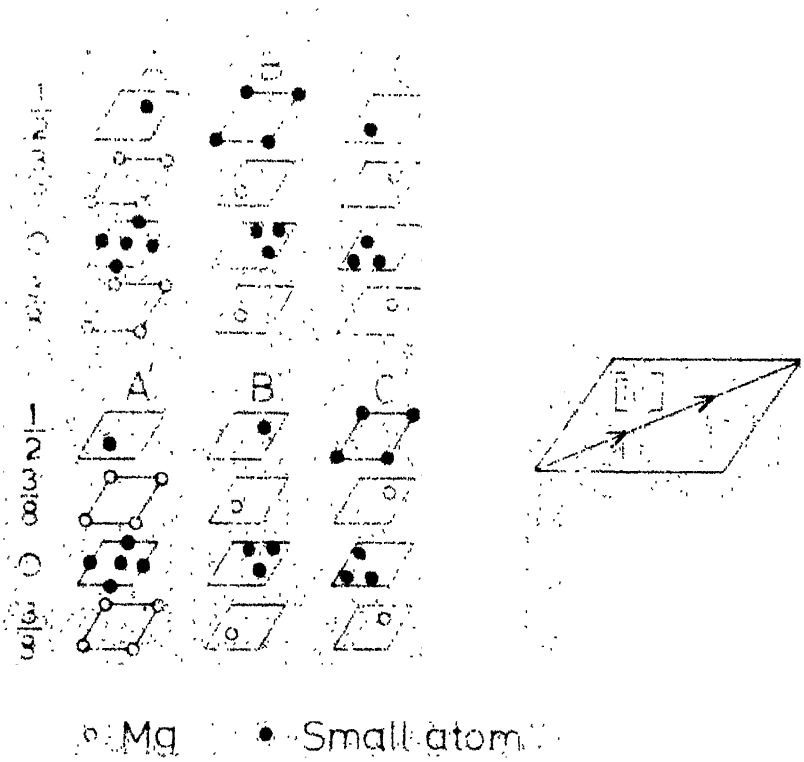

Fig. 8 Possible ways of the layer stacking

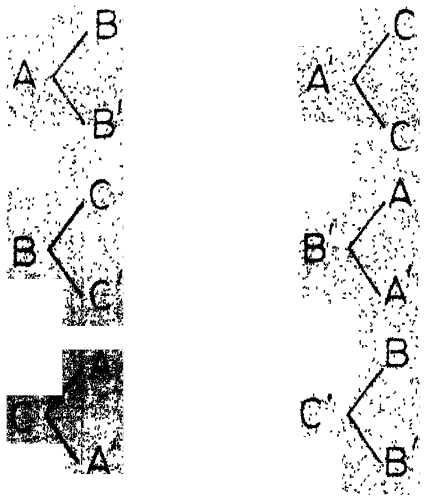

Fig. 9. Alloy No.1 (Mo-Fe-Si)
Micrograph shows three phases: Small grains are distinctly visible in contrast to grains of third phase. Background shows the matrix magnification X1000.

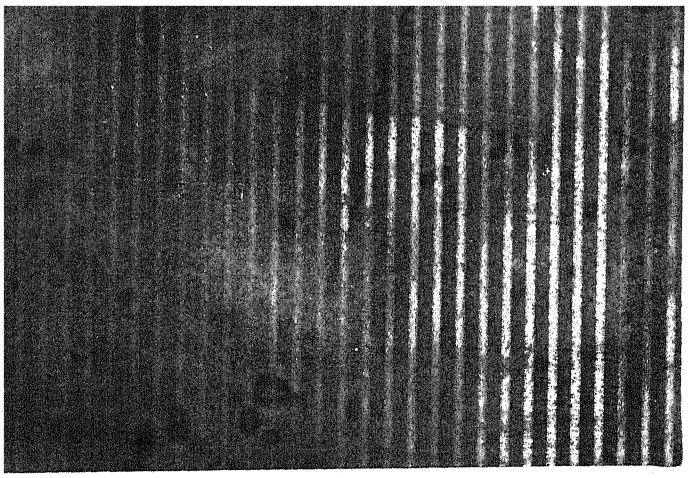

Fig.10. Alloy No. 8 (Mo-Fe-Si)
Micrograph shows two phases: black spots

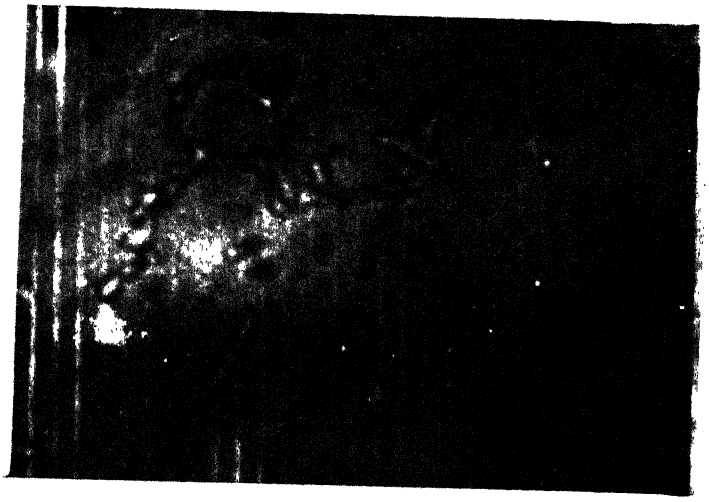

Fig.11. Alloy No. 22 (Mo-Fe-Si)

Micrograph shows two phases: precipitates are seen somewhat in chain shape in the background of matrix. Magnification X1000.

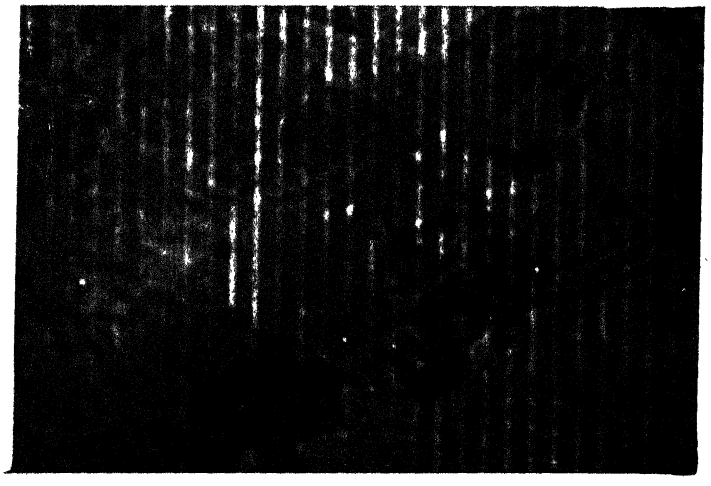

Fig.12. Alloy No. 32 (Mo-Fe-Si)

Micrograph shows two phases. Magnification 1000X.

Fig. 13. Alloy No. 1 (Mo-Co-Si)
Micrograph shows three phases.
Magnification 1000X.

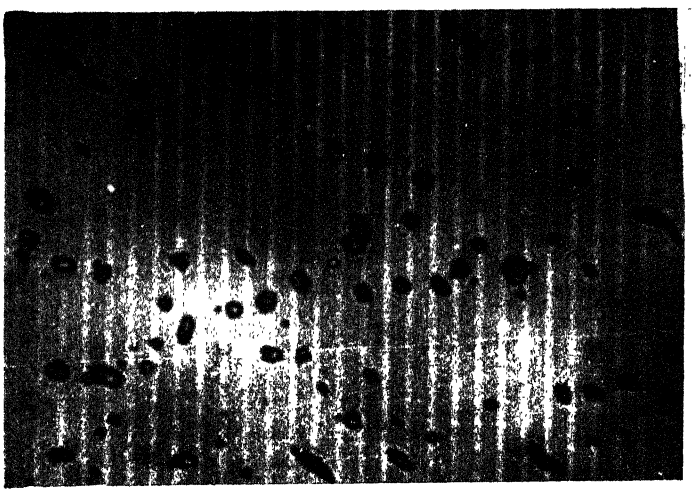

Fig.14. Alloy No. 16 (Mo-Co-Si)
Micrograph shows two phases: precipitates are seen as black spots arranged in some systematic way in the background of matrix.
Magnification X1000.

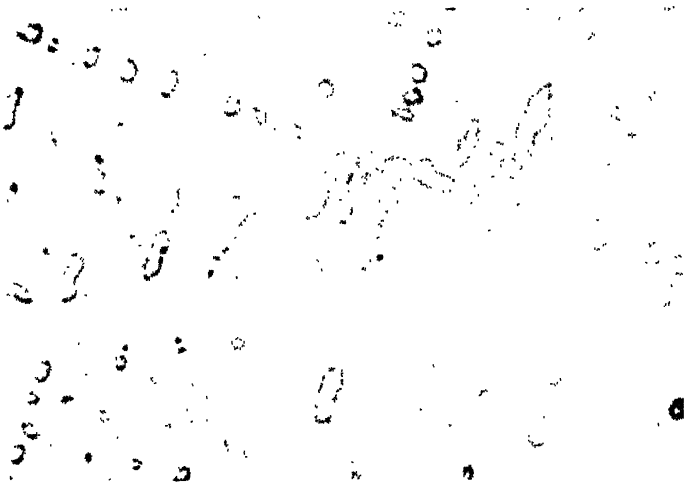

Fig. 15. Alloy No. 21 (Mo-Co-Si)
Micrograph shows two phases: precipitates μ are seen in the background of matrix. Magnification X1000.

Fig.16. Alloy No.23 (Mo-Co-Si)
Micrograph shows two phases: precipitates ε_1 are seen somewhat segregrated in the background of matrix. Magnification X1000

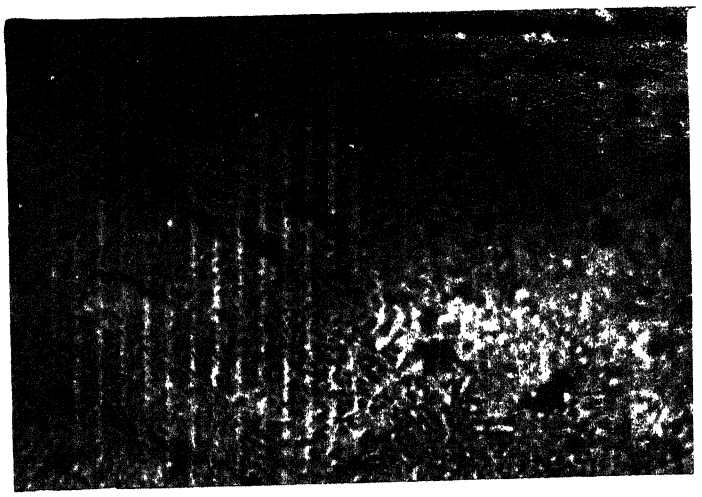

Fig. 17. Alloy No. 32 (Mo-Co-Si)
Micrograph shows two phase and finely dispersed second phase precipitates are seen.

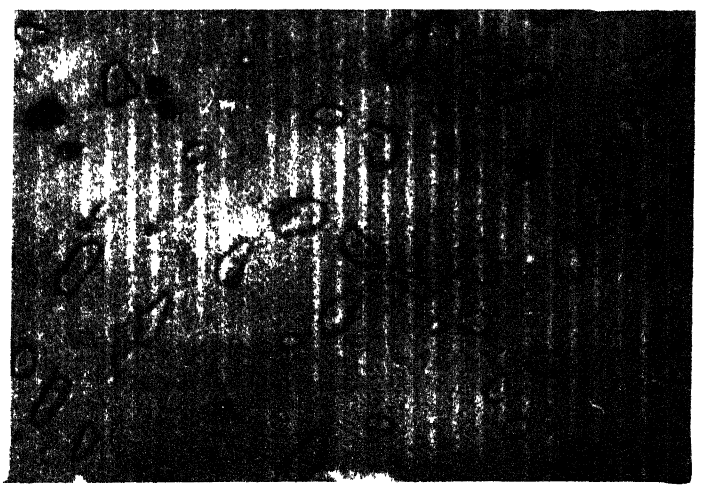

Fig. 18. Alloy No. 1 (Mo-Ni-Si)
Micrograph shows two phases: Precipitates are seen distributed more or less uniformly in the background of matrix. Third phase is not visible. Magnification X1000.

Fig. 19. Alloy No. 25 (Mo-Ni-Si)

Micrograph shows three phases: Two phases are not quite distinct from each other but are well separated together frombackground of matrix. Magnification X1000.

Fig. 20. Alloy No. 26 (Mo-Ni-Si)

Micrograph shows three phases: Second phase is seen as black spots. Third phase is seen as darker inthe background of matrix. Magnification X1000.

Fig. 21. Alloy No.27 (Mo-Ni-Si)

Micrograph shows three phases: Precipitates, second and third phases are seen separated from background of matrix. Third phase is quite distinct within second phase. Magnification X1000.

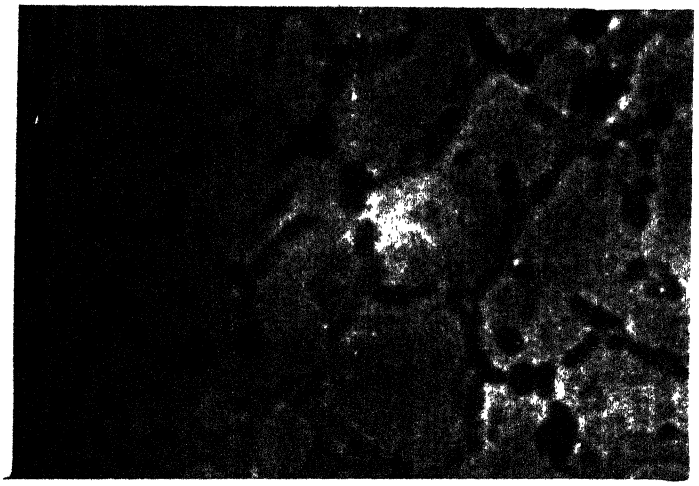

Fig.22. Alloy No. 29 (Mo-Ni-Si)

Micrograph shows three phases: second phase is seen as dark nets. Third phase lies in background alongwith matrix. Magnification X1000.

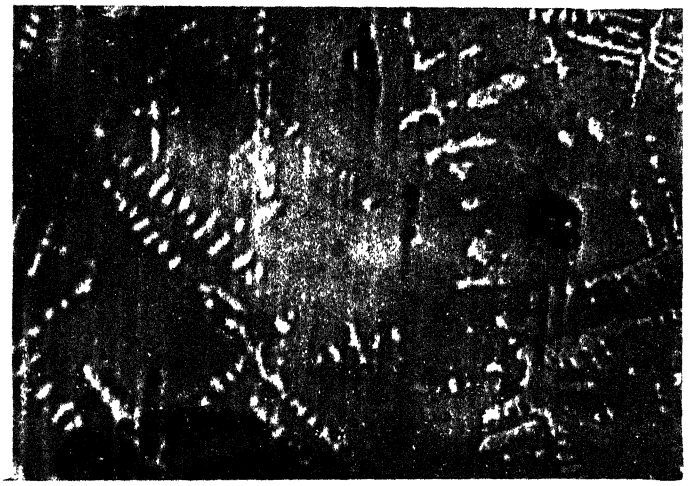

Fig.23. Alloy No. 37 (Mo-Ni-Si)

Micrograph shows two phases: Precipitate phase is seen in form of dendrites in the background of matrix. Magnification X1000.

Date Slip

This book is to be returned on the date last stamped.

.....	.....
.....	.....
.....	.....
.....	.....
.....	.....
.....	.....
.....	.....
.....	.....
.....	.....
.....	.....
.....	.....

CD 6.72.9